

NASA CR-172,485

NASA Contractor Report 172485

ICASE REPORT NO. 84-56

NASA-CR-172485  
19850006490

# ICASE

COMPARISON OF UNIFORM PERTURBATION SOLUTIONS AND  
NUMERICAL SOLUTIONS FOR SOME POTENTIAL FLOWS PAST  
SLENDER BODIES

FOR INFORMATION

NOT TO BE USED FOR REPRODUCTION

Tin-Chee Wong  
C. H. Liu  
James Geer

Contract No. NAS1-17070  
October 1984

LIBRARY COPY

JAN 15 1985

LANGLEY RESEARCH CENTER  
LIBRARY, NASA  
HAMPTON, VIRGINIA

INSTITUTE FOR COMPUTER APPLICATIONS IN SCIENCE AND ENGINEERING  
NASA Langley Research Center, Hampton, Virginia 23665

Operated by the Universities Space Research Association

**NASA**

National Aeronautics and  
Space Administration

Langley Research Center  
Hampton, Virginia 23665



COMPARISON OF UNIFORM PERTURBATION SOLUTIONS AND NUMERICAL SOLUTIONS  
FOR SOME POTENTIAL FLOWS PAST SLENDER BODIES

Tin-Chee Wong  
George Washington University

C. H. Liu  
NASA Langley Research Center

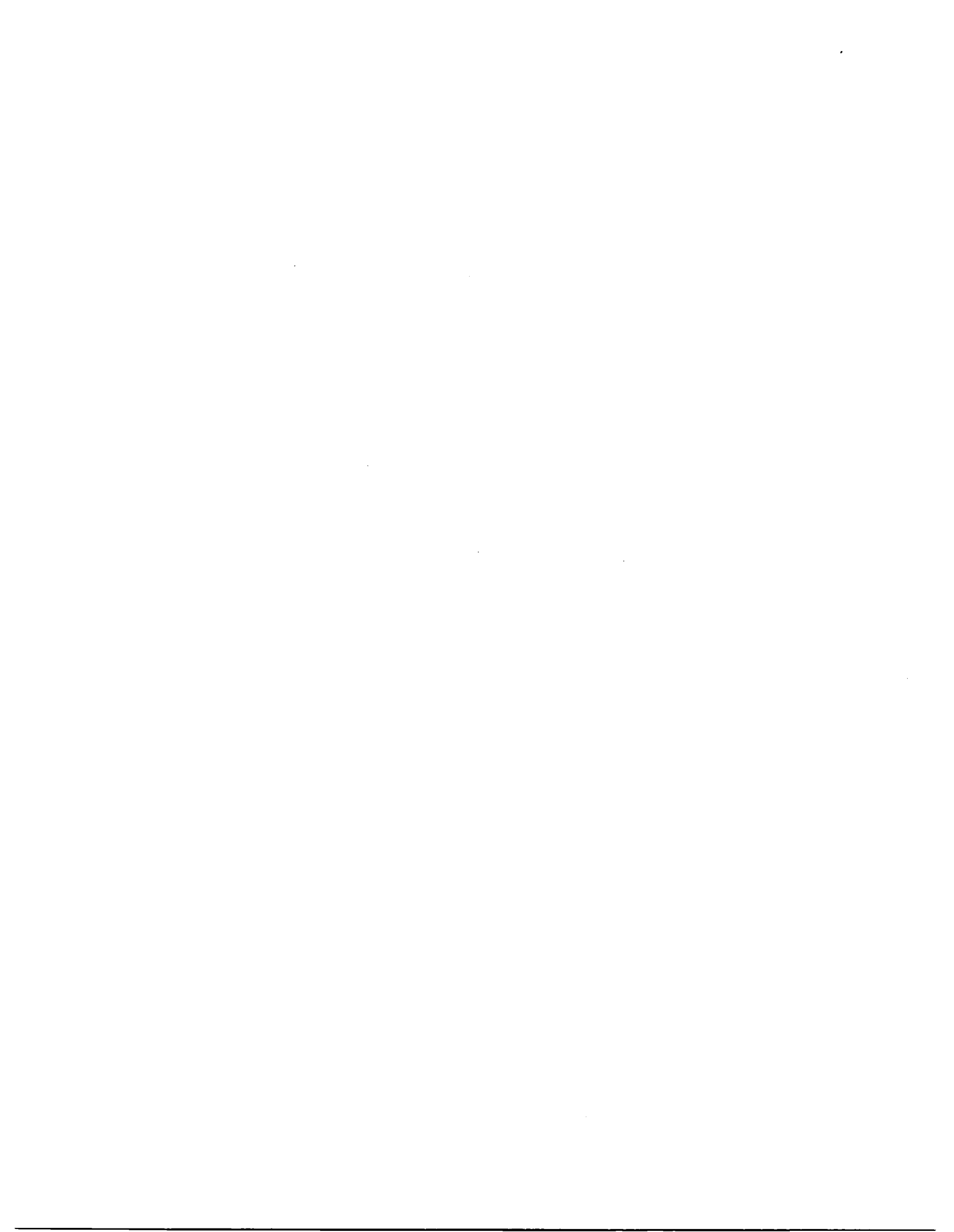
James Geer  
State University of New York at Binghamton

Abstract

Approximate solutions for potential flow past an axisymmetric slender body and past a thin airfoil are calculated using a uniform perturbation method and then compared with either the exact analytical solution or the solution obtained using a purely numerical method. The perturbation method is based upon a representation of the disturbance flow as the superposition of singularities distributed entirely within the body, while the numerical (panel) method is based upon a distribution of singularities on the surface of the body. It is found that the perturbation method provides very good results for small values of the slenderness ratio and for small angles of attack. Moreover, for comparable accuracy, the perturbation method is simpler to implement, requires less computer memory, and generally uses less computation time than the panel method. In particular, the uniform perturbation method yields good resolution near the regions of the leading and trailing edges where other methods fail or require special attention.

---

Research was supported by the National Aeronautics and Space Administration under NASA Contract No. NAS1-14605 for the first author and under NASA Contract No. NAS1-17070 for the third author while he was in residence at the Institute for Computer Applications in Science and Engineering, NASA Langley Research Center, Hampton, VA 23665.



## Introduction

Many different methods have been developed to obtain an approximate solution to potential flow problems involving fixed finite bodies. For a few very special cases, analytical methods can be used to obtain an exact solution to the exterior flow problem. However, in most cases, usually due to the geometric complexity of the problem, approximate methods must be employed. Two of the more widely used approximate methods are perturbation methods and numerical methods. Perturbation methods take advantage of the fact that many shapes of practical interest are either slender or thin and hence certain simplifications can be made in the problem formulation. Many numerical methods are based on the idea of approximating the body as a collection of "simpler" shapes (e.g., panels) and then satisfying an appropriate boundary condition on each of these simpler shapes. The primary purpose of this paper concerns the results of comparing the approximate solutions obtained by a uniform perturbation method and a standard numerical method (and exact solutions, where they exist) to a variety of potential flow problems involving either a slender body of revolution or a thin airfoil.

The perturbation method we shall use is based upon an approach suggested by Handelsman and Keller [1] and developed more fully by Geer and Keller [2] and Geer [3,4]. This method represents the part of the potential due to the body as the superposition of potentials due to distributed point singularities. These singularities lie entirely within the body. The boundary condition on the surface of the body then leads to an integral equation for the density of the singularity distribution. This equation can be solved asymptotically as the slenderness ratio of the body approaches zero. By demanding that the resulting asymptotic expansion be regular, the

extent of the singularity distribution within the body can also be determined. Thus, this method leads to an approximate solution for the flow field which is uniformly valid over the entire surface of the body, including the ends (e.g., nose and tail) of the body. Hence, as we shall see, it can easily be used to compute the surface velocity (and hence the pressure coefficient) on the body surface.

The numerical method we shall use is commonly referred to as a "panel method" (see, e.g., Maskew [5]). Here the body is approximated by a finite number of panels (or line segments, in two dimensions). Then the flow due to the presence of the body is represented by a distribution of singularities over these elements, with a polynomial variation of the density of the distribution over each element. The boundary condition on the body surface then leads to a system of algebraic equations for the polynomial coefficients.

In Sections 2 and 3, below, the specific problems that we shall consider are formulated, and the uniform asymptotic solutions are presented. Surface pressure coefficients computed from the perturbation and numerical methods are presented in Section 4, while our results are discussed in Section 5.

## **2. Flow Past an Axisymmetric Slender Body**

In this section and the next, we shall formulate two classes of potential flow problems that we shall consider in detail. In particular, these include flow past a slender body of revolution and the flow over a thin two-dimensional airfoil. For each class of problems, we will summarize the general uniform perturbation method of solution and present the relevant formulas. We shall then apply the results to some specific examples.

Consider the problem of determining the steady potential flow past a slender body of revolution (see Figure 1). We fix a cylindrical coordinate system  $(r, \theta, x)$  within the body, with the  $x$ -axis coinciding with the axis of the body and the origin at one end of the body, and assume, for simplicity, that the incident flow is a uniform flow with speed  $U$  parallel to the axis of the body. Then the surface of the body can be described by  $r = \epsilon \sqrt{S(x)}$  for  $0 \leq x \leq 1$ . Here  $\epsilon$  is called the slenderness ratio of the body and is defined as the ratio of the maximum radius of the body to its length  $L$ . The function  $S(x)$ , which satisfies  $\max S(x) = 1$  for  $0 \leq x \leq 1$ , is a prescribed function which describes the shape of the body, with  $\pi \epsilon^2 S(x)$  being the cross-sectional area of the body at the station  $x$ . Here we have non-dimensionalized all lengths by referring them to  $L$ .

To determine the flow about this body, we represent the part of the potential due to the body as the superposition of potentials due to point sources distributed along the axis of the body and lying entirely inside the body. Thus, we write the potential  $\phi$  as

$$\phi = U \left\{ x - \frac{1}{4\pi} \int_{\alpha}^{\beta} \frac{f(\xi, \epsilon)}{\sqrt{(x - \xi)^2 + r^2}} d\xi \right\}. \quad (2.1)$$

Here  $f(\xi, \epsilon)$  is the (unknown) density of the source distribution, while  $\alpha$  and  $\beta$ , which depend upon  $\epsilon$  and are also unknown, determine the extent of the distribution within the body. They satisfy the inequalities  $0 < \alpha < \beta < 1$ ; (see Figure 1).

The potential defined by (2.1) satisfies Laplace's equation outside the body and reduces to the uniform flow potential at infinity. The boundary condition that the normal component of the flow velocity must vanish on the surface of the body, when used with (2.1), leads to the requirement

$$\epsilon^2 S^-(x) = \frac{1}{2\pi} \frac{d}{dx} \int_{\alpha}^{\beta} \frac{(x - \xi)}{\sqrt{(x - \xi)^2 + \epsilon^2 S(x)}} f(\xi, \epsilon) d\xi. \quad (2.2)$$

Equation (2.2) is an integral equation for the density of the source distribution, from which  $f(\xi, \epsilon)$ , as well as  $\alpha$  and  $\beta$ , can be determined.

For small values of  $\epsilon$ , the integral operator on the right side of (2.2) can be expanded asymptotically as a power series in  $\epsilon^2$  and a power series in  $\epsilon^2$  multiplied by  $\log(\epsilon^2)$ . The coefficients in these series can be expressed as certain linear operators applied to the density function  $f(\xi, \epsilon)$ ; (see, e.g., Handelsman and Keller [1] for details). The form of this expansion suggests that the solution for  $f(\xi, \epsilon)$  can be expressed in the form

$$\begin{aligned} f(x, \epsilon) = & \epsilon^2 f_{10}(x) + \epsilon^4 f_{20}(x) + \epsilon^4 \log \epsilon^2 f_{21}(x) + \epsilon^6 f_{30}(x) \\ & + \epsilon^6 \log \epsilon^2 f_{31}(x) + \epsilon^6 (\log \epsilon^2)^2 f_{32}(x) + O(\epsilon^8 \log \epsilon^2), \end{aligned} \quad (2.3)$$

where each of the functions  $f_{n,m}(x)$  is independent of  $\epsilon$ . By substituting (2.3) into the expanded form of (2.2) and equating the coefficients of like terms in  $\epsilon$ , the functions  $f_{n,m}(x)$  can be determined recursively. In particular,

$$f_{10}(x) = \pi S'(x),$$

$$f_{20}(x) = -\frac{\pi}{4} \frac{d}{dx} \left\{ \frac{SS'}{x} - \frac{SS'}{1-x} - SS'' + SS'' \log \left[ \frac{4x(1-x)}{S(x)} \right] \right. \\ \left. + S \int_0^{1-x} \{S'(x+v) - S'(x) - vS''(x)\} v^{-2} dv \right. \\ \left. - S \int_0^x \{S'(x-v) - S'(x) + vS''(x)\} v^{-2} dv \right\}$$

$$f_{21}(x) = \frac{\pi}{4} (SS'')', \quad f_{30}(x) = 0$$

$$f_{31}(x) = \frac{1}{4} \left\{ \frac{d}{dx} (Sf_{20}') - \frac{1}{8} \frac{d}{dx} (S^2 f_{10}'') - \frac{d}{dx} (f_{21}' [S \log \left[ \frac{4x(1-x)}{S} \right] - S] \right. \\ \left. + f_{21} \left( \frac{S}{x} - \frac{S}{1-x} \right) \right) + S \int_0^x \{f_{21}(x-v) - f_{21}(x) + vf_{21}'(x)\} v^{-2} dv \\ \left. - S \int_0^{1-x} \{f_{21}(x+v) - f_{21}(x) - vf_{21}'(x)\} v^{-2} dv \right\}$$

$$f_{32}(x) = \frac{\pi}{16} \frac{d}{dx} \left\{ S \frac{d^2}{dx^2} (SS'') \right\}. \quad (2.4)$$

By demanding that each of the coefficient functions  $f_{n,m}(x)$  is regular on  $0 \leq x \leq 1$ , Handelsman and Keller [1] were able to show that  $\alpha(\epsilon)$  and  $\beta(\epsilon)$  can be expressed in the form

$$\alpha = \alpha(\epsilon) = \sum_{n=1}^{\infty} \alpha_n \epsilon^{2n}, \quad \beta = \beta(\epsilon) = 1 - \sum_{n=1}^{\infty} \beta_n \epsilon^{2n} \quad (2.5)$$

where the coefficients  $\alpha_n$  and  $\beta_n$  can be expressed in terms of  $S(x)$ . In particular, they showed that

$$\alpha = \frac{c_1}{4} \epsilon^2 - \frac{c_1 c_2}{16} \epsilon^4 + \frac{c_1(c_1 c_3 + 2c_2^2)}{64} \epsilon^6 + O(\epsilon^8), \quad c_j = S^{(j)}(0)/j! \quad (2.6)$$

$$\beta = 1 - \frac{d_1}{4} \epsilon^2 + \frac{d_1 d_2}{16} \epsilon^4 - \frac{d_1(d_1 d_3 + 2d_2^2)}{64} \epsilon^6 + O(\epsilon^8), \quad d_j = (-1)^j S^{(j)}(1)/j! \quad (2.7)$$

Thus, once  $S(x)$  is specified,  $\alpha$  and  $\beta$  can be determined from (2.6)-(2.7) and then used in (2.1), along with the expression (2.3) for  $f(x, \epsilon)$ , to yield the asymptotic expansion of the potential with an accuracy of  $O(\epsilon^8 \log \epsilon^2)$ .

As applications of these results, we consider two specific examples. These are:

- 1) Ellipsoid of revolution, for which

$$S(x) = 4x(1 - x), \text{ (Figures 2a,b);}$$

- 2) "Dumbbell" shaped body, for which

$$S(x) = 4bx(1 - x)[1 - bx(1 - x)], \quad b > 2, \text{ (Figures 3a,b).}$$

When these specific formulas for  $S(x)$  are used in (2.4), (2.6), and (2.7), and then these results are used in (2.1), an explicit expression for the flow potential is obtained for each example. In Section 4 we shall use these formulas to compute the pressure coefficient on the surface of each body and then compare these results with the pressure coefficient found by using an exact solution and/or the panel method.

### 3. Flow Past a Thin Airfoil

Consider now the problem of determining the steady potential flow about a thin airfoil which is immersed in an otherwise uniform flow field. We introduce an  $x,y$ -cartesian coordinate system fixed in the airfoil (see Figure 4) and let the surface of the airfoil be described by  $y = \epsilon [C(x) \pm \sqrt{S(x)}]$  for  $0 \leq x \leq 1$ . (Here we have again nondimensionalized  $x$  and  $y$  by referring all lengths to the chord  $L$  of the airfoil.) The parameter  $\epsilon$  is called the slenderness parameter of the body, where  $C(x)$  and  $S(x)$  are prescribed functions describing the camber line and thickness profile, respectively, of the airfoil. In particular, for an airfoil that is symmetric about the  $x$ -axis,  $C(x) = 0$ .

To determine the flow potential  $\phi$  about the airfoil, it is convenient to think of  $\phi$  as the real part of a complex potential  $\Phi(z)$ , which is an analytic function (outside the airfoil) of the complex variable  $z = x + iy$ . Then we represent the part of the potential due to the body as the superposition of potentials due to (complex) point sources distributed along an arc which lies entirely within the body (see Figure 4). Thus, we set

$$\phi(z) = U\left\{e^{-i\gamma} z - \frac{1}{2\pi} \int_{\alpha}^{\beta} \log(z - \xi) f(\xi, \epsilon) d\xi\right\}, \quad (3.1)$$

where  $f(\xi, \epsilon)$  is the (unknown) density of the source distribution while  $\alpha$  and  $\beta$ , which are also unknown, determine the extent of the distribution within the body. The parameter  $\gamma$  represents the angle of the uniform stream makes with the positive x-axis (i.e., the angle of attack). The real part of this expression satisfies Laplace's equation outside the airfoil and reduces to the uniform flow potential at infinity.

The only remaining condition to be satisfied is the vanishing of the normal component of the velocity on the body's surface. This condition, when used with (3.1), leads to a pair of coupled integral equations for the (complex) source density  $f(\xi, \epsilon)$ , from which  $\alpha$  and  $\beta$  can also be determined. The case of a symmetric airfoil ( $C(x) = 0$ ) was analyzed by Geer and Keller [2], while the general case of a cambered airfoil was studied in detail by Geer [3]. Using the results of these investigators, we find that for small values of the slenderness parameter  $\epsilon$ ,

$$f(z, \epsilon) = \frac{1}{\sqrt{(\beta - z)(z - \alpha)}} \{f_0(z) + f_1(z)\epsilon + f_2(z)\epsilon^2 + O(\epsilon^3)\}, \quad (3.2)$$

where,

$$f_0(x) = i\left(\frac{\Gamma_0}{\pi} + (2x - 1)\sin\gamma\right)$$

$$\operatorname{Re}f_1(x) = -\frac{1}{2\pi}\sqrt{\frac{x(1-x)}{S(x)}}\{2\pi S'(x)\cos\gamma + \operatorname{Re}L_1^1(f_0(x))\}$$

$$\operatorname{Im}f_1(x) = \tilde{f}_1(x) + \frac{\Gamma_1}{\pi} - \frac{2}{\pi}\int_0^{\frac{\pi}{2}}\tilde{f}_1(\sin^2\theta)d\theta$$

$$\begin{aligned}\tilde{f}_1(x) &= \frac{x}{2\pi}\{\operatorname{Im}L_1^0(f_0(x)) - 4\pi C'(x)\cos\gamma\} \\ &\quad - \frac{x}{\pi^2}\int_0^{\frac{\pi}{2}}\frac{\cos^2\theta}{\sin^2\theta - x}\{\operatorname{Im}L_1^0(f_0(\xi)) - 4\pi C'(\xi)\cos\gamma\}\Bigg|_{\xi=x}^{\xi=\sin^2\theta}d\theta\end{aligned}$$

$$\operatorname{Re}f_2(x) = -\frac{1}{2\pi}\sqrt{\frac{x(1-x)}{S(x)}}\{\operatorname{Re}L_1^1(f_1(x)) + \operatorname{Re}L_2^1(f_0(x))\}$$

$$\operatorname{Im}f_2(x) = \tilde{f}_2(x) + \frac{\Gamma_2}{\pi} - \frac{2}{\pi}\int_0^{\frac{\pi}{2}}\{\tilde{f}_2(\sin^2\theta) + \frac{\sin\gamma}{2}(S'(0)\cos^2\theta + S'(1)\sin^2\theta)\}d\theta$$

$$\begin{aligned}\tilde{f}_2(x) &= \frac{x}{2\pi}\{\operatorname{Im}L_1^0(f_1(x)) + \operatorname{Im}L_2^0(f_0(x))\} \\ &\quad - \frac{x}{\pi^2}\int_0^{\frac{\pi}{2}}\frac{\cos^2\theta}{\sin^2\theta - x}\{\operatorname{Im}L_1^0(f_1(\xi)) + \operatorname{Im}L_2^0(f_0(\xi))\}\Bigg|_{\xi=x}^{\xi=\sin^2\theta}d\theta\end{aligned}\quad (3.3)$$

and  $\alpha$  and  $\beta$  are given by

$$\alpha = \alpha(\epsilon) = \frac{1}{4} d_1 \epsilon^2 - \frac{1}{4} c_1 d_1 \epsilon^3 - \frac{1}{16} d_1 (d_2 + 4c_1^2) \epsilon^4 + O(\epsilon^5)$$

$$\beta = \beta(\epsilon) = 1 - \frac{1}{4} \tilde{d}_1 \epsilon^2 - \frac{1}{4} \tilde{c}_1 \tilde{d}_1 \epsilon^3 + \frac{1}{16} \tilde{d}_1 (\tilde{d}_2 + 4\tilde{c}_1^2) \epsilon^4 + O(\epsilon^5)$$

$$c_j = c^{(j)}(0)/j!; d_j = s^{(j)}(0)/j!; \tilde{c}_j = (-1)^j c^{(j)}(1)/j!; \tilde{d}_j = (-1)^j s^{(j)}(1)/j! \quad (3.4)$$

In (3.3),  $L_j^k$  are certain linear operators which are defined by Geer [3]. The constants  $\Gamma_j$  are related to the total circulation  $\Gamma(\epsilon)$  about the airfoil by  $\Gamma(\epsilon) = \Gamma_0 + \Gamma_1 \epsilon + \Gamma_2 \epsilon^2 + O(\epsilon^3)$ . If the airfoil has a sharp trailing edge at  $z = 1$ , then Geer [3] has shown that the Kutta condition leads to the requirement that  $\text{Im}f_j(1) = 0$  for each  $j$ . Hence the constants  $\Gamma_j$  are determined uniquely for this case from the formulas (3.3). Thus, once  $C(x)$  and  $S(x)$  have been specified, they can be used in (3.2)-(3.4) and then these results inserted into (3.1) to yield an approximate expression for the flow potential which has an accuracy of  $O(\epsilon^3)$ .

As applications of these results, we consider two specific examples. These are the:

- 1) Symmetric second-order Joukowski airfoil, for which

$$C(x) = 0 \quad \text{and} \quad S(x) = x(1 - x)^3; \quad (\text{Figures 5a,b}).$$

- 2) Cambered second-order Joukowski airfoil, for which

$$C(x) = ax(1 - x) \quad \text{and} \quad S(x) = x(1 - x)^3; \quad (\text{Figures 6a-d}).$$

In the next section, we will use the formulas above to compute the surface pressure coefficient for these examples, with different angles of attack.

#### 4. Comparison of Perturbation and Numerical Results

In this section we shall compare the results of using the perturbation formulas of the previous two sections and a low-order panel method code (see, e.g., Maskew [5]) to compute the pressure coefficient  $C_p$  on the surface of a slender body of revolution or a thin airfoil. These results will also be compared with those obtained from an exact analytical solution to the flow problem, when such a solution is available. In particular, using Bernoulli's equation, we find

$$C_p = (2/\rho U^2)(p - p_\infty) = 1 - U^{-2} |\vec{V}\phi|^2, \quad (4.1)$$

where  $\rho$  is the density of the fluid,  $p$  is the fluid pressure on the body surface,  $p_\infty$  is the pressure at infinity, and the velocity  $\vec{V}\phi$  is evaluated on the surface of the body.

In Figures 2a,b, we compare the pressure coefficient on a slender ellipsoid of revolution computed from the exact solution (see, e.g., Lamb [6]), the uniform perturbation solution presented in Section 2, and the panel method (using 300 panels). The length-to-diameter ratios for the two examples considered are 5 and 2.5, which correspond to values of  $\epsilon = 0.1$  and  $\epsilon = 0.2$ , respectively. We note that there is in general good agreement between the two approximate methods of solution and that the uniform perturbation method gives very good accuracy near the ends of the body, where non-uniform perturbation methods often fail (see, e.g., Van Dyke [7]).

Some results for the dumbbell shaped body are presented in Figures 3a,b. Here the perturbation method is extended only up to terms which are  $O(\epsilon^4)$ , while 300 panels are still used in the panel method. The profile parameter  $b$  is chosen to be 3, while two different values of  $\epsilon$  are considered. As the figures indicate, for small values of  $\epsilon$ , the two methods agree well. Observe that, for these examples, as well as several other similar cases we considered, each perturbation solution required only about 2 seconds of computing time, while each panel method computation required 5 seconds (for 180 panels) or 14 seconds (for 300 panels). All computations were performed on a CDC Cyber 173.

The perturbation and panel method solutions for a symmetric second-order Joukowski airfoil are compared for two different values of  $\epsilon$  and an angle of attack of  $6^\circ$  in Figures 5a,b. The panel method experiences some difficulty in resolving the flow field near the leading edge of the airfoil, while the uniform perturbation method produces a smooth solution. (This difficulty was even more evident, in other cases we considered, as the angle of attack was increased or the slenderness ratio decreased). In Table I, the lift coefficients for several different cases are calculated using these two methods and compared with the "exact" lift coefficient for this airfoil (see Karamcheti [8]). From this table, we see that the perturbation method produces a more accurate lift coefficient for the cases considered than does the panel method.

The pressure coefficients  $C_p$  on a second-order cambered Joukowski airfoil with two different thickness-to-chord ratios and two different angles of attack are presented in Figures 6a-d. The perturbation method is carried to terms which are  $O(\epsilon^2)$ , while the number of panels is 50 for each case.

The corresponding lift coefficients are summarized in Table II and compared with the "exact" solution for these cases. From Table II it is clear that the panel method produces more accurate results for thicker airfoils, while the uniform perturbation results are more accurate as the slenderness ratio is decreased or as the angle of attack is increased. This observation is consistent with the fact that the panel method again has difficulty in resolving the flow near the leading edge of the airfoil. For these examples, about 8 seconds of computing time were required for each perturbation solution, while about 5 seconds were required for each panel method computation.

## 5. Discussion

The examples and results displayed here have shown that the uniform perturbation method can be used to describe accurately some aerodynamic characteristics for slender bodies of revolution and for thin airfoils. When compared with the exact solutions available, the results of several cases similar to those presented here show that the perturbation solutions tend to become more accurate as the number of terms in the perturbation expansion is increased, which suggests that the perturbation solutions are convergent series, at least up to some maximum value of  $\epsilon$ .

The uniform perturbation method is designed to provide an accurate description of the flow field over the entire surface of a smooth slender body, including the ends of the body. The panel method experiences some difficulty in a region near the leading edge of a thin airfoil (which could be corrected, of course, with the addition of more panels in this region or by a

high-order panel method). This inaccuracy in the flow description leads to a less accurate prediction of the lift coefficient. For thicker bodies of revolution or thicker airfoils, this problem is less pronounced and, in fact, the panel method gives more accurate results than does the (truncated) perturbation expansion we have used here. Thus, we find that the panel and uniform perturbation methods nicely complement each other, with the uniform perturbation solution providing a more accurate description of the flow for very slender bodies and the panel method being more accurate for thicker bodies.

In addition to the accuracy considerations just mentioned, it should be emphasized that the perturbation method often requires less computer storage and execution time than does the panel method. The primary mathematical operations involved in the computation of the perturbation solution are simply some functional evaluations and numerical integrations. Since relatively little storage is required for these computations, they could be performed on a microcomputer, although we have made no effort to carry out our calculations in this manner.

Our studies demonstrate that the uniform perturbation method can be used to provide low-cost, accurate solutions to flow problems involving slender bodies. Because of their low cost, these solutions could also be used effectively to provide qualitatively reliable solutions in the initial stages of design efforts for even thicker bodies of revolution and airfoils, with the panel method being used only when more accuracy is required.

### References

1. R. A. Handelsman and J. B. Keller, Axially symmetric potential flow around a slender body. J. Fluid Mech. 28, 131-147 (1967).
2. J. F. Geer and J. B. Keller, Uniform asymptotic solutions for potential flow around a thin airfoil and the electrostatic potential about a thin conductor. SIAM J. Appl. Math. 16, 75-101 (1968).
3. J. F. Geer, Uniform asymptotic solutions for the two-dimensional potential field about a slender body. SIAM J. Appl. Math. 26, 539-553 (1974).
4. J. F. Geer, Uniform asymptotic solutions for potential flow about a slender body of revolution. J. Fluid Mech. 67, 817-827 (1975).
5. B. Maskew, Predicting of subsonic aerodynamic characteristics - a case for low-order panel methods. AIAA 19th Aero. Sci. Mtg., Paper no. AIAA 81-0252 (1981).
6. H. Lamb, Hydrodynamics, 6th Edition. Dover Publications, New York (1945).
7. M. Van Dyke, Perturbation Methods in Fluid Mechanics. Parabolic Press, Stanford (1975).
8. K. Karamcheti, Principles of Ideal Fluid Aerodynamics. Wiley, New York (1966).

**Table I:** Comparison of values for the lift coefficient for a symmetric Joukowski airfoil with different slenderness ratios and angles of attack using the exact, perturbation, and panel methods.

Slenderness ratio $\epsilon$	Exact $C_{l,ex}$	Perturbation $C_{l,pt}$	Panel $C_{l,pn}$	$\frac{C_{l,pt} - C_{l,ex}}{C_{l,ex}} \times 100\%$	$\frac{C_{l,pn} - C_{l,ex}}{C_{l,ex}} \times 100\%$
$\gamma = 6^\circ$					
0.01624	0.67278	0.67319	0.63080	0.06	-6.24
0.03248	0.68797	0.68961	0.65377	0.24	-4.97
0.04872	0.70234	0.70603	0.66472	0.53	-5.36
0.06496	0.71588	0.72245	0.67684	0.92	-5.45
$\gamma = 12^\circ$					
0.01624	1.33819	1.33901	1.23750	0.06	-7.52
0.03248	1.36840	1.37167	1.29823	0.24	-5.13
0.04872	1.39698	1.40432	1.32128	0.53	-5.42
0.06496	1.42391	1.43698	1.34485	0.92	-5.55

Table II: Comparison of values for the lift coefficient for a cambered Joukowski airfoil with different slenderness ratios and angles of attack using the exact, perturbation, and panel methods.

Slenderness ratio $\epsilon$	Exact $C_{l,ex}$	Perturbation $C_{l,pt}$	Panel $C_{l,pn}$	$\frac{C_{l,pt} - C_{l,ex}}{C_{l,ex}} \times 100\%$	$\frac{C_{l,pn} - C_{l,ex}}{C_{l,ex}} \times 100\%$
			$\gamma = 0^\circ$		
0.02688	0.15689	0.16101	0.14812	2.62	-5.59
0.05376	0.31268	0.32987	0.30390	5.50	-2.81
0.08064	0.46641	0.50658	0.46610	8.61	-0.07
0.10752	0.61721	0.69115	0.63346	11.98	2.63
			$\gamma = 6^\circ$		
0.02688	0.82841	0.83332	0.77878	0.59	-5.99
0.05376	0.99734	1.01767	0.95359	2.04	-4.39
0.08064	1.16264	1.20984	1.12378	4.06	-3.34
0.10752	1.32350	1.40981	1.29947	6.52	-1.82
			$\gamma = 12^\circ$		
0.02688	1.49084	1.49649	1.38619	0.38	-7.02
0.05376	1.67107	1.69432	1.58984	1.39	-4.86
0.08064	1.84614	1.89984	1.76670	2.91	-4.30
0.10752	2.01528	2.11303	1.94816	4.85	-3.33

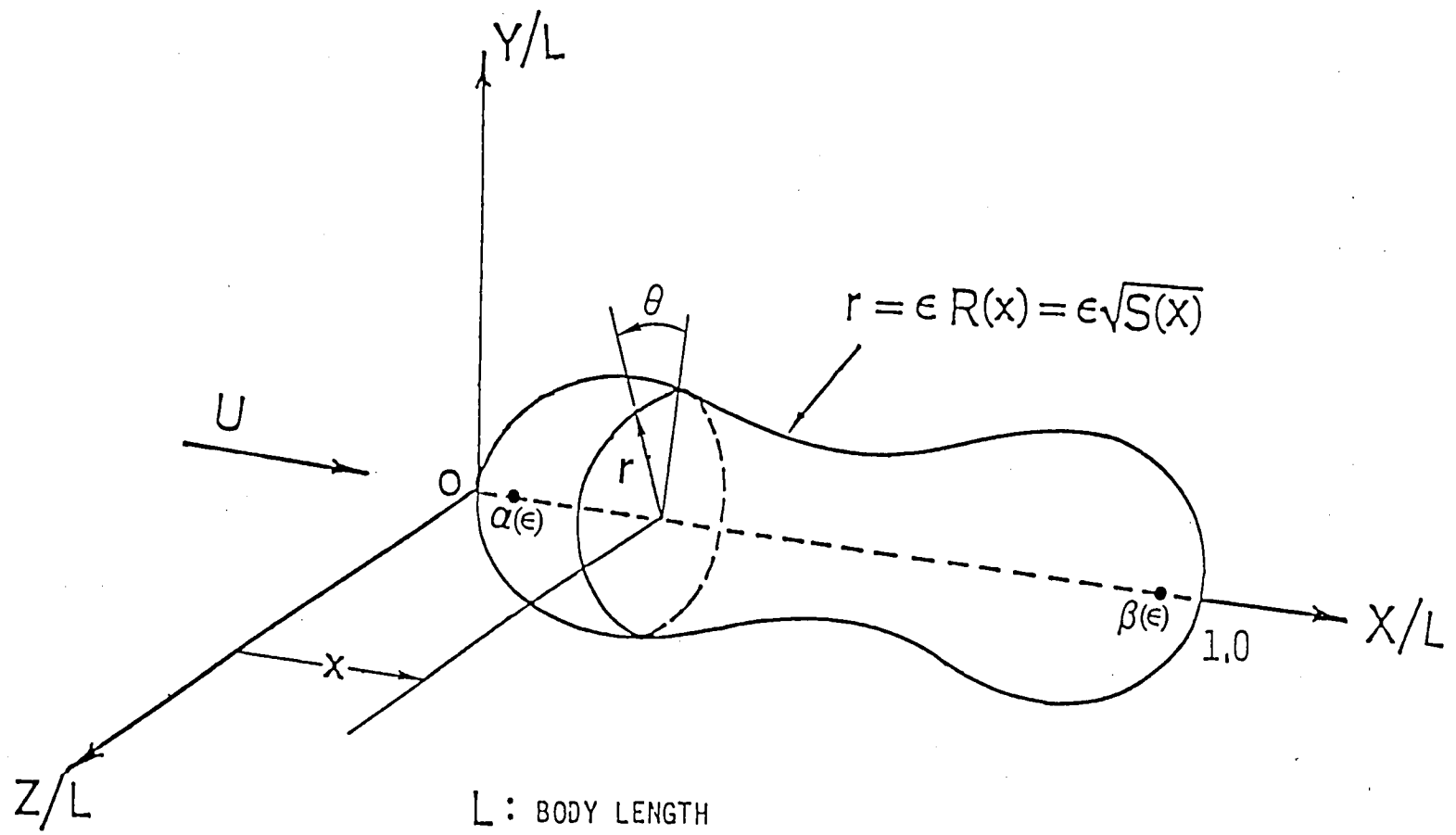


Figure 1

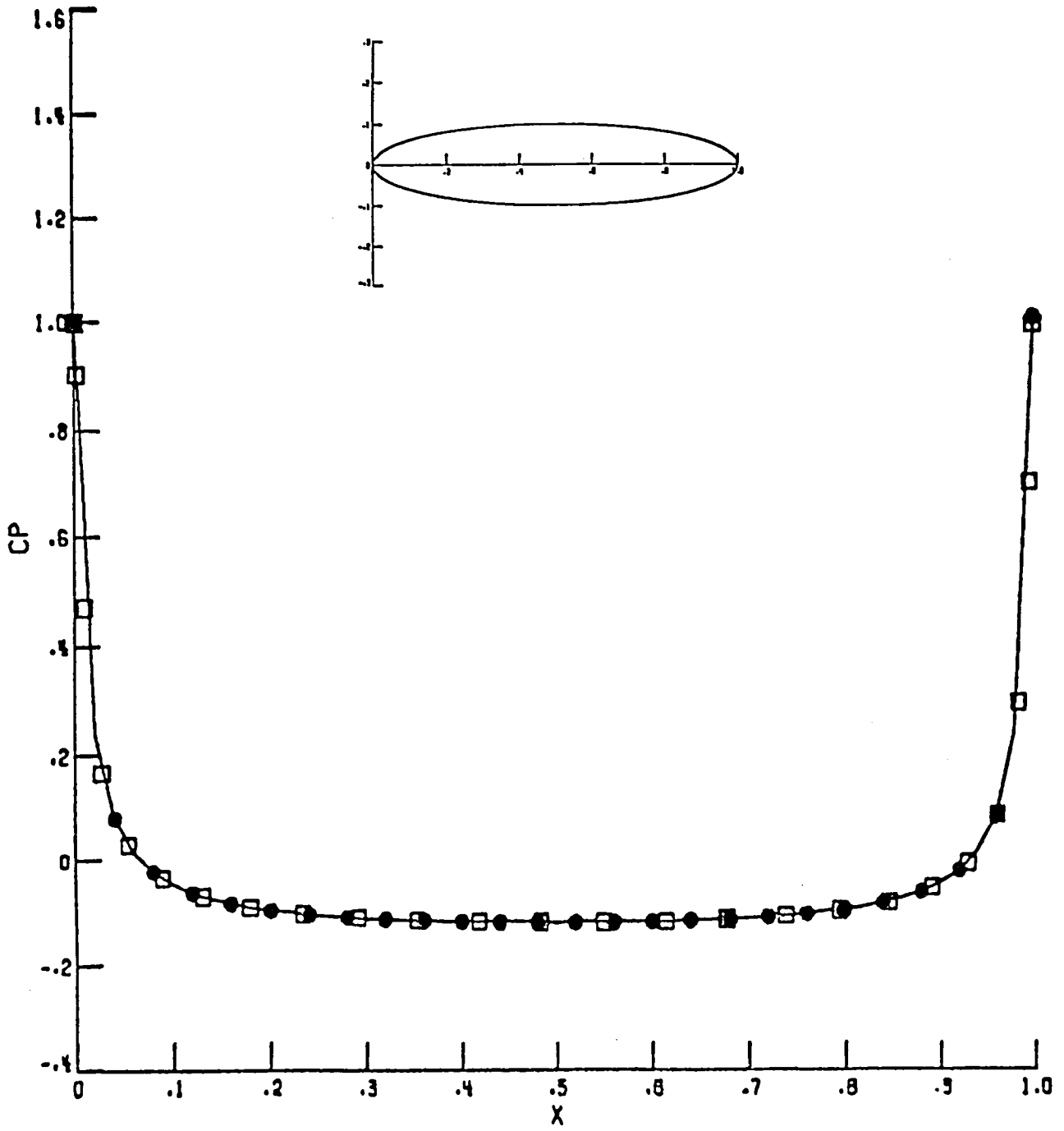


Figure 2a

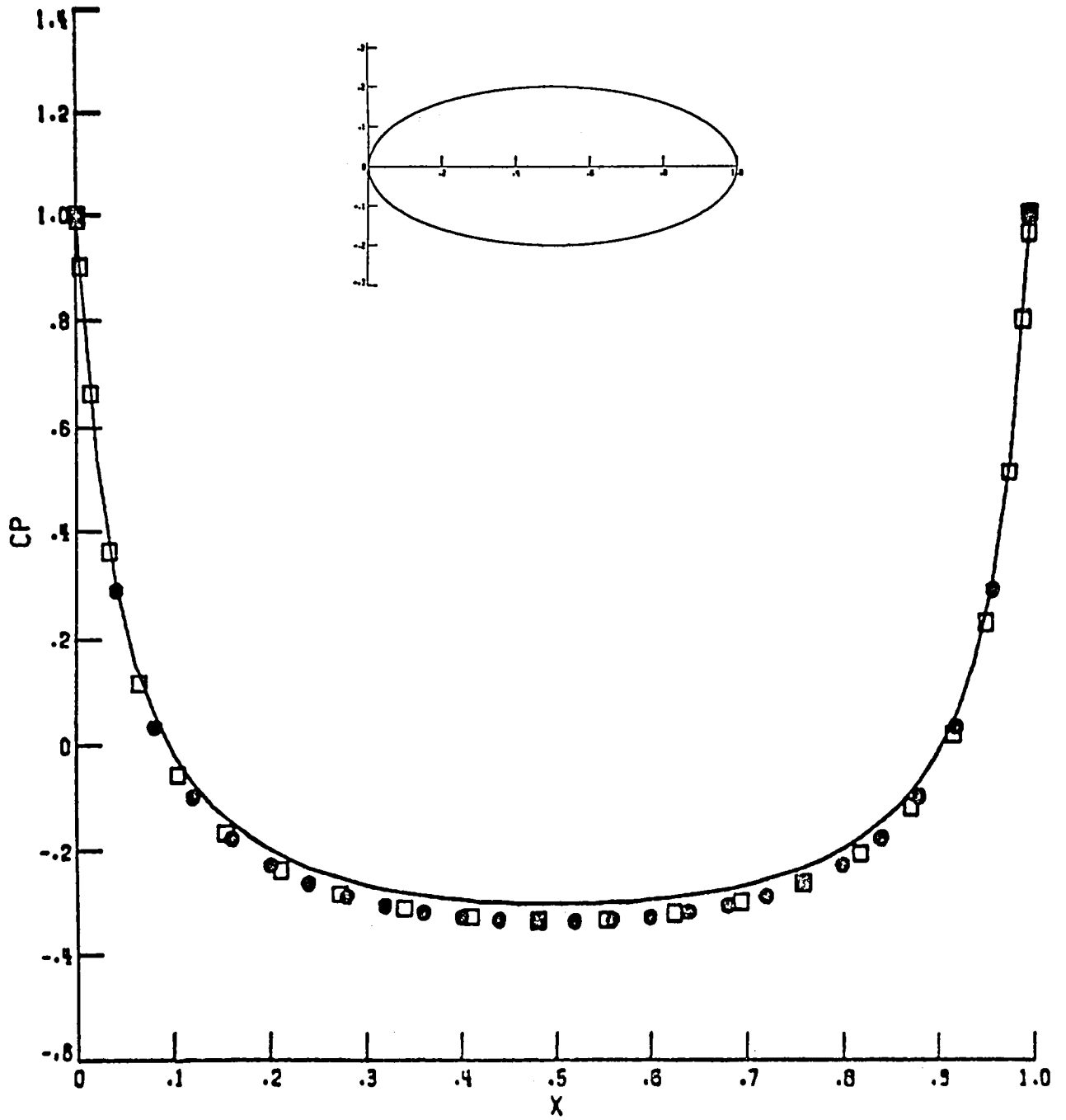


Figure 2b

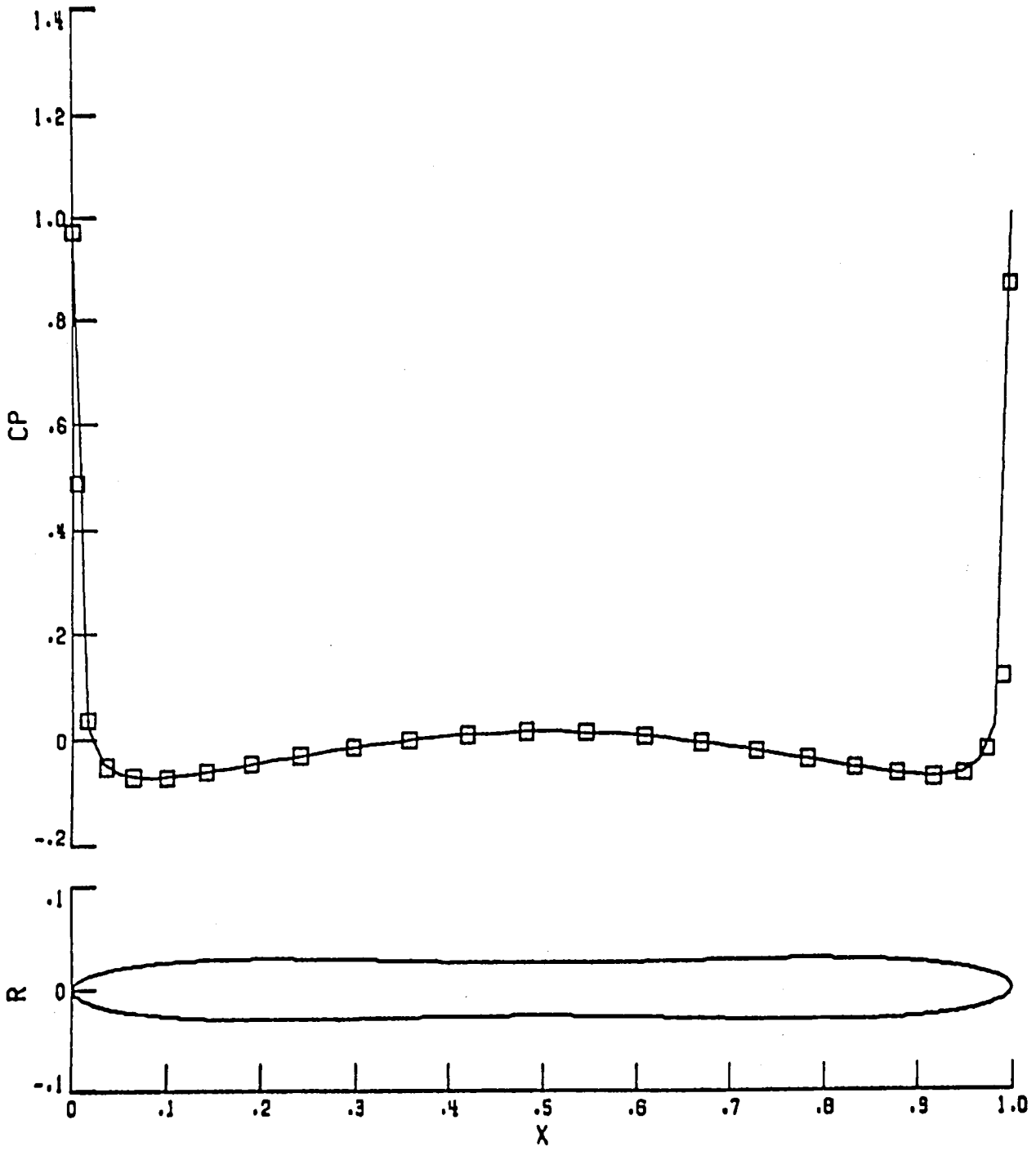


Figure 3a

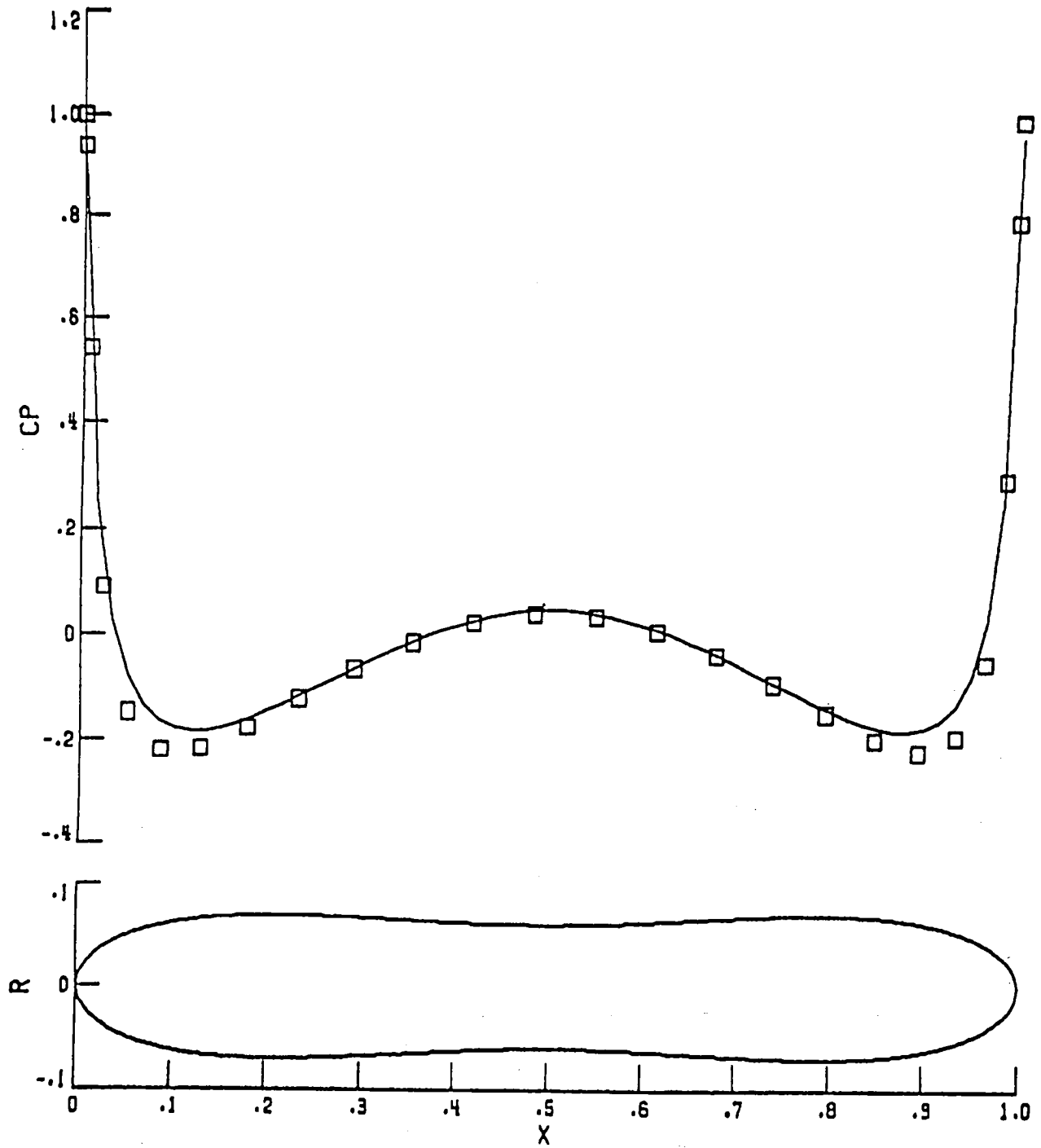


Figure 3b

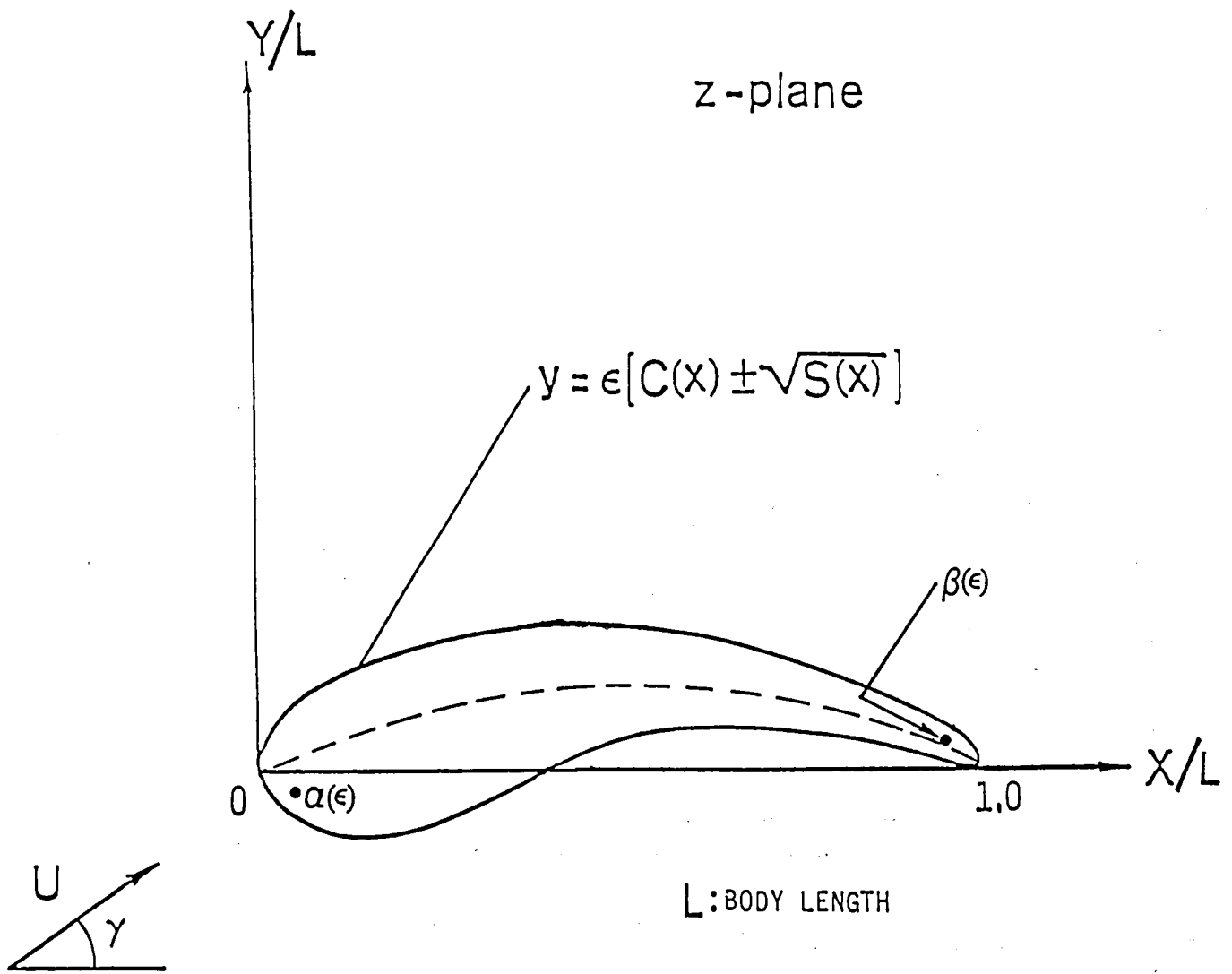


Figure 4

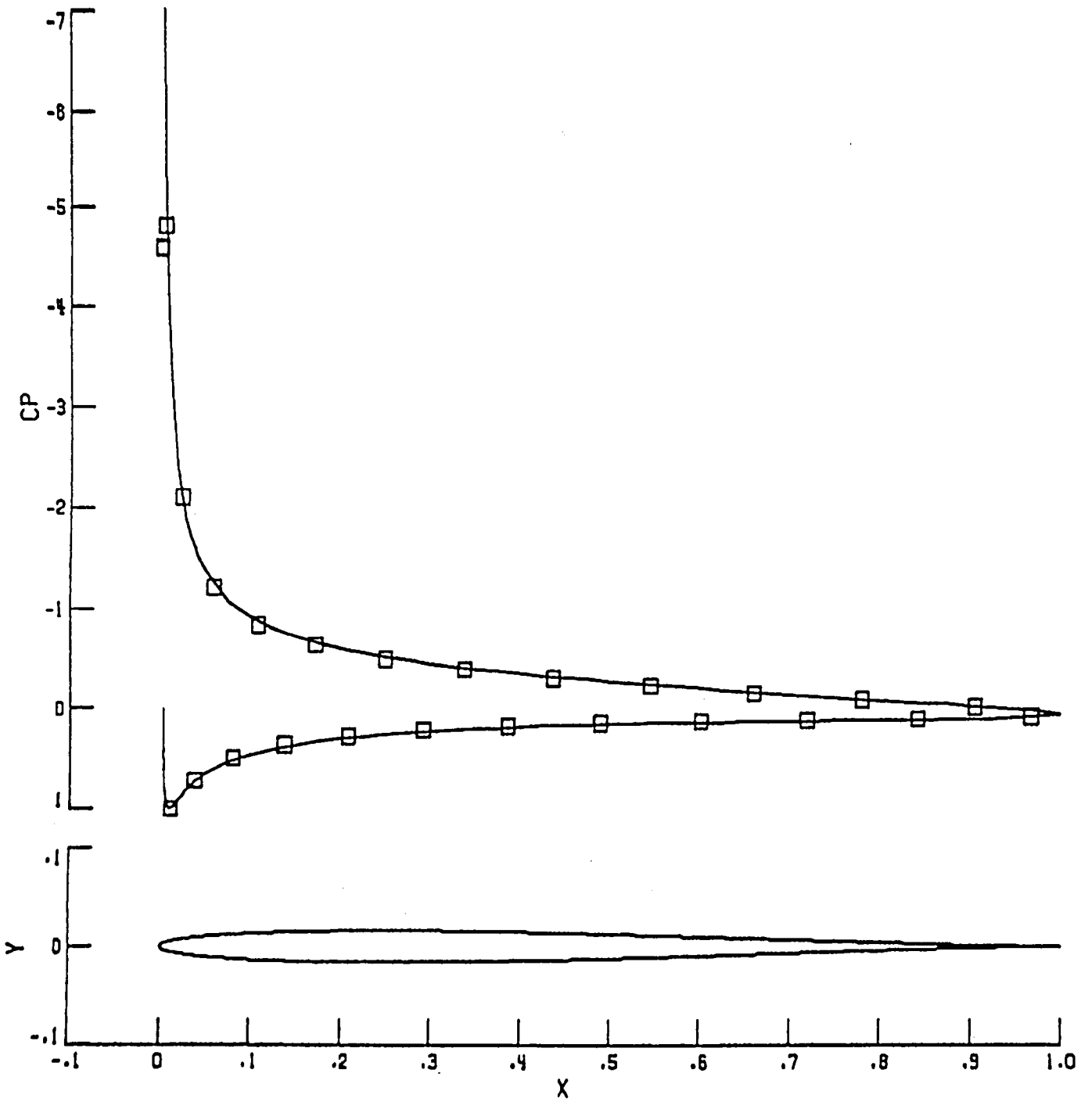


Figure 5a

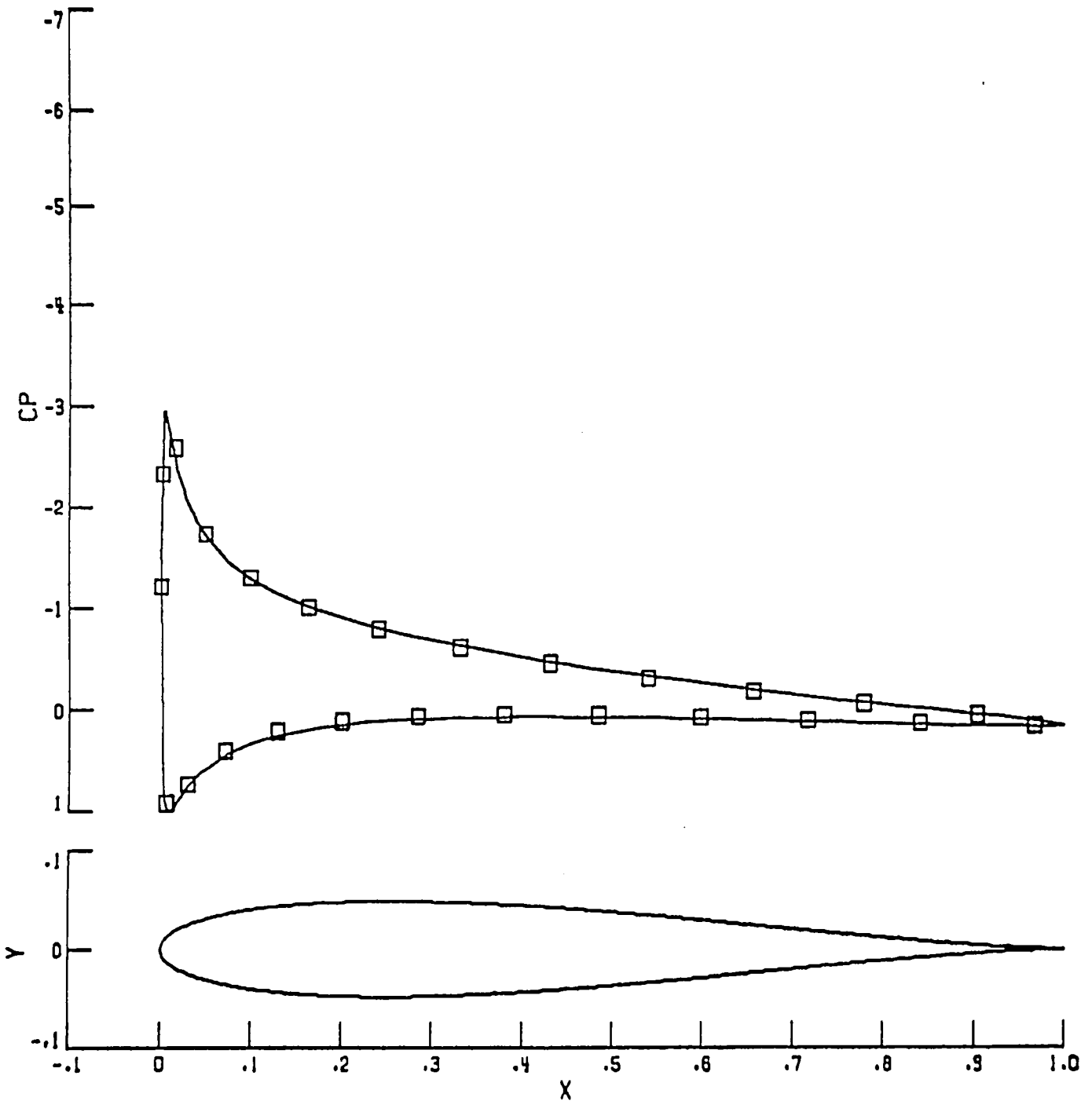


Figure 5b

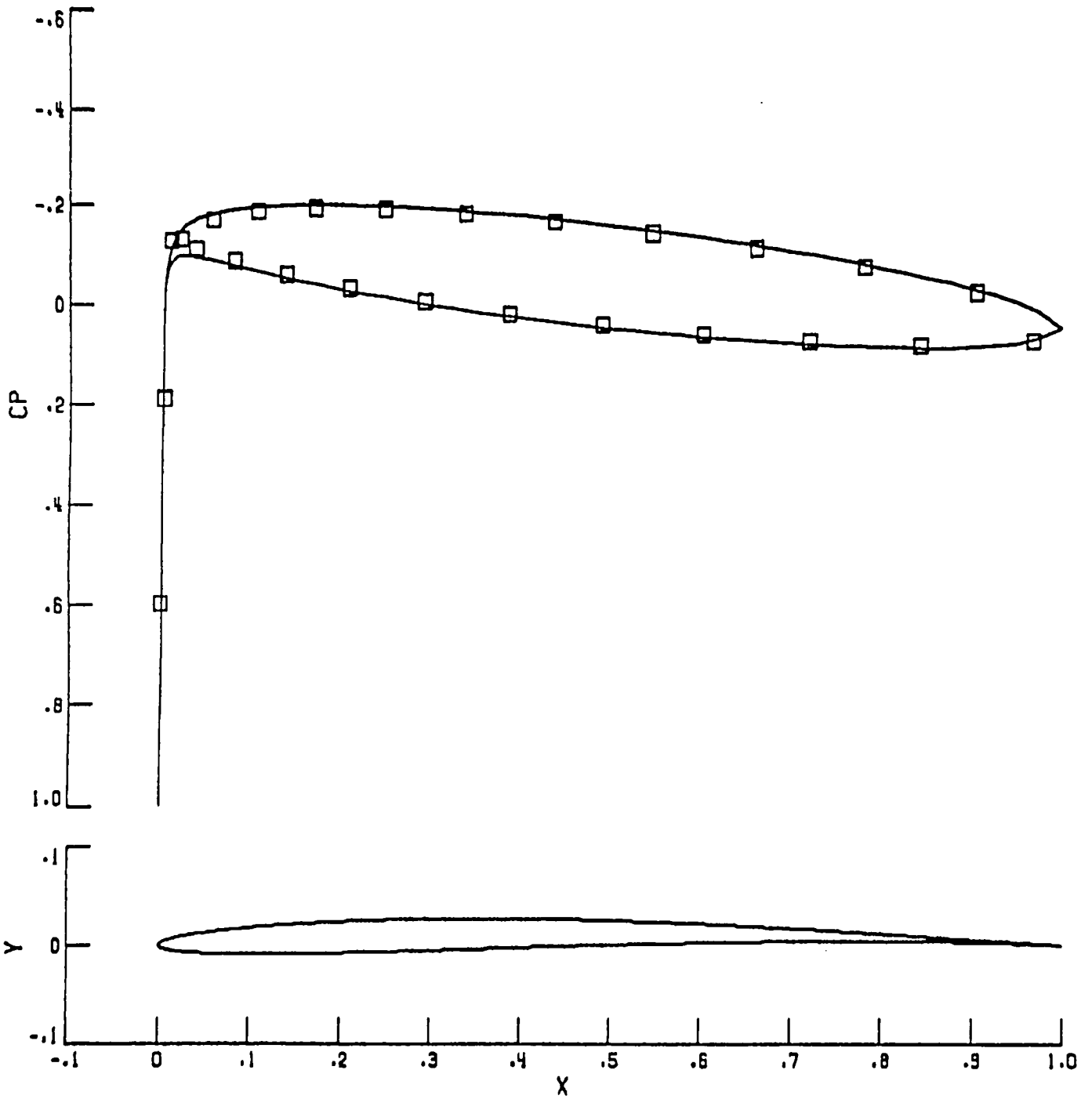


Figure 6a

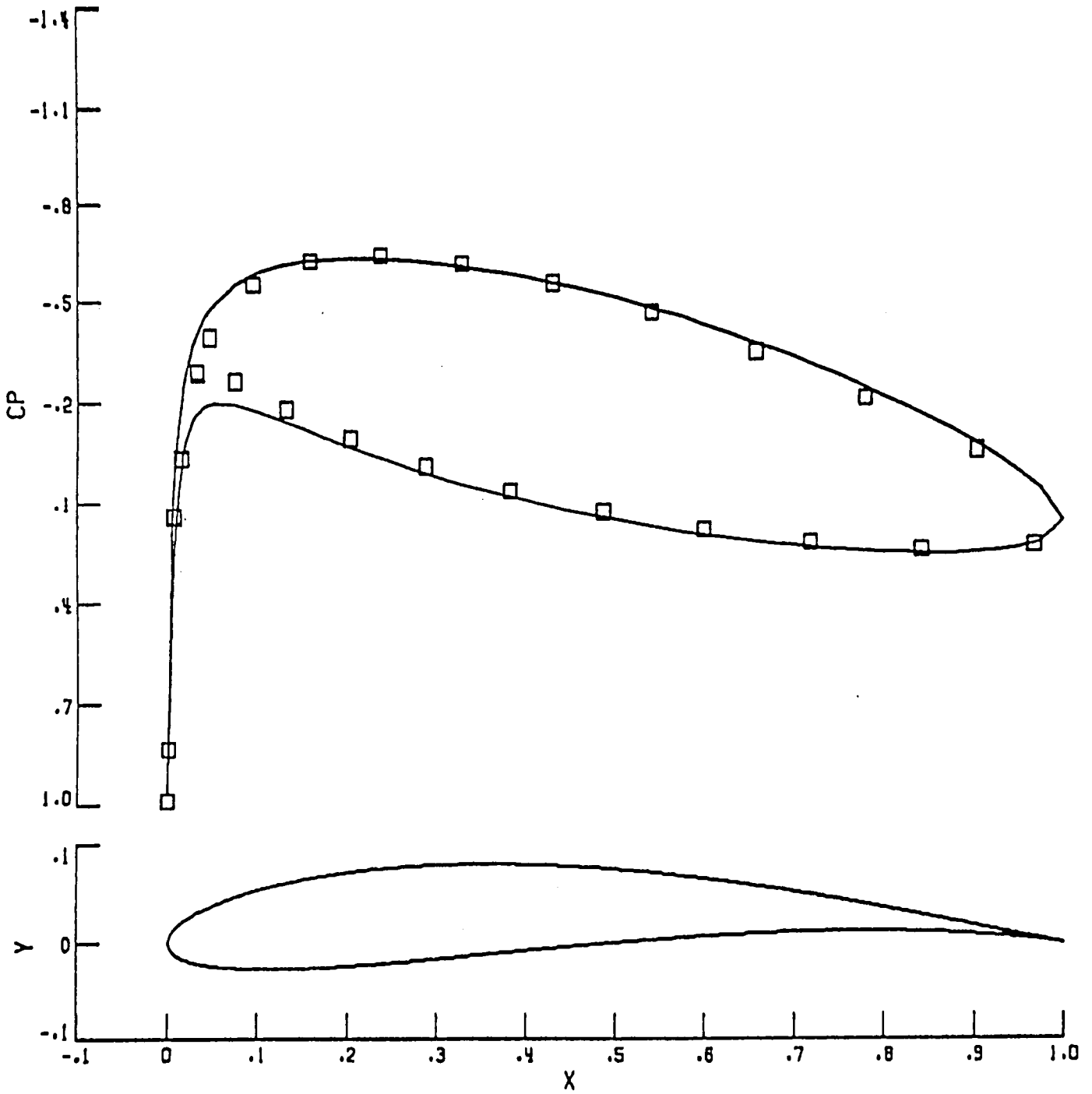


Figure 6b

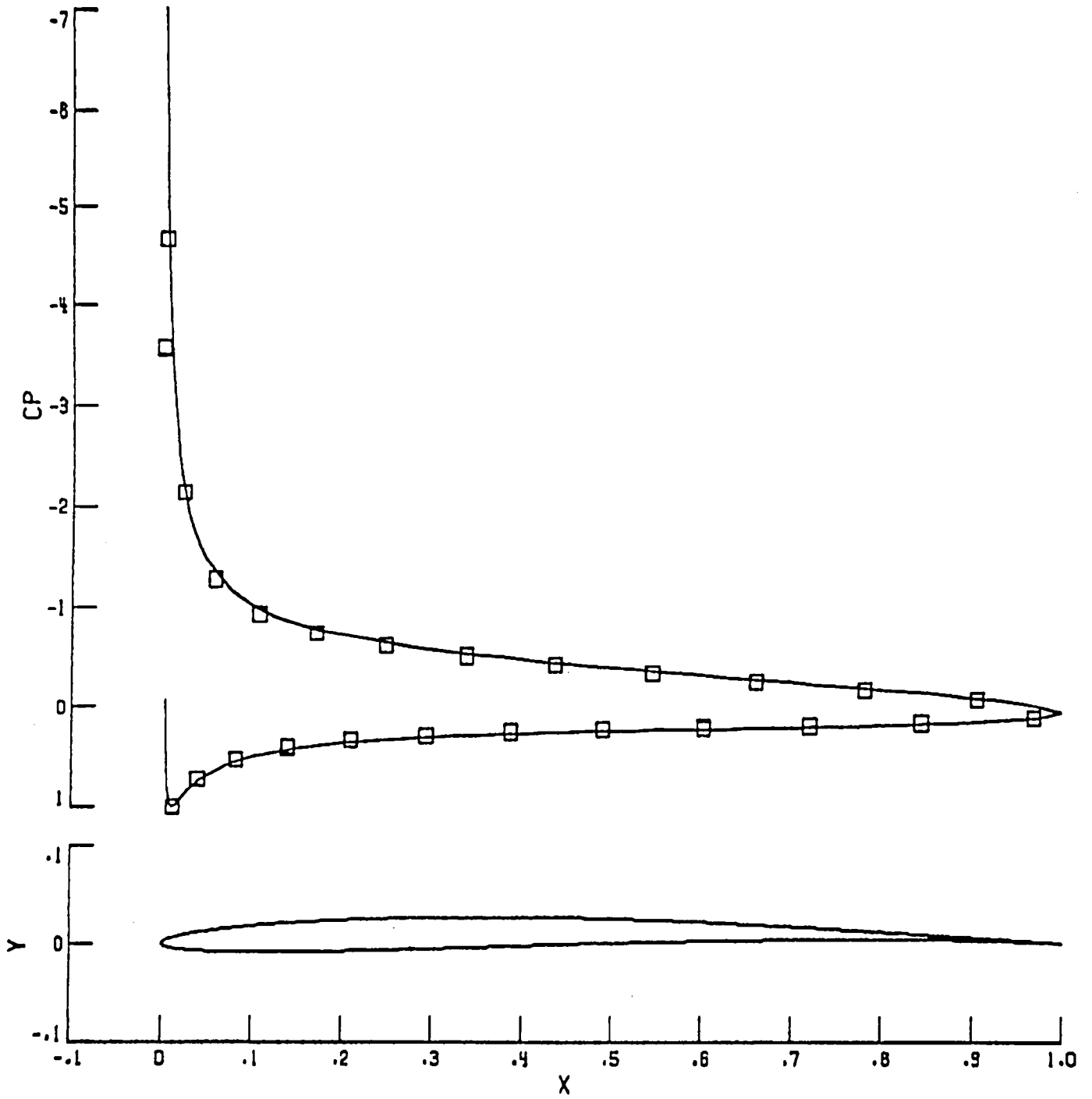


Figure 6c

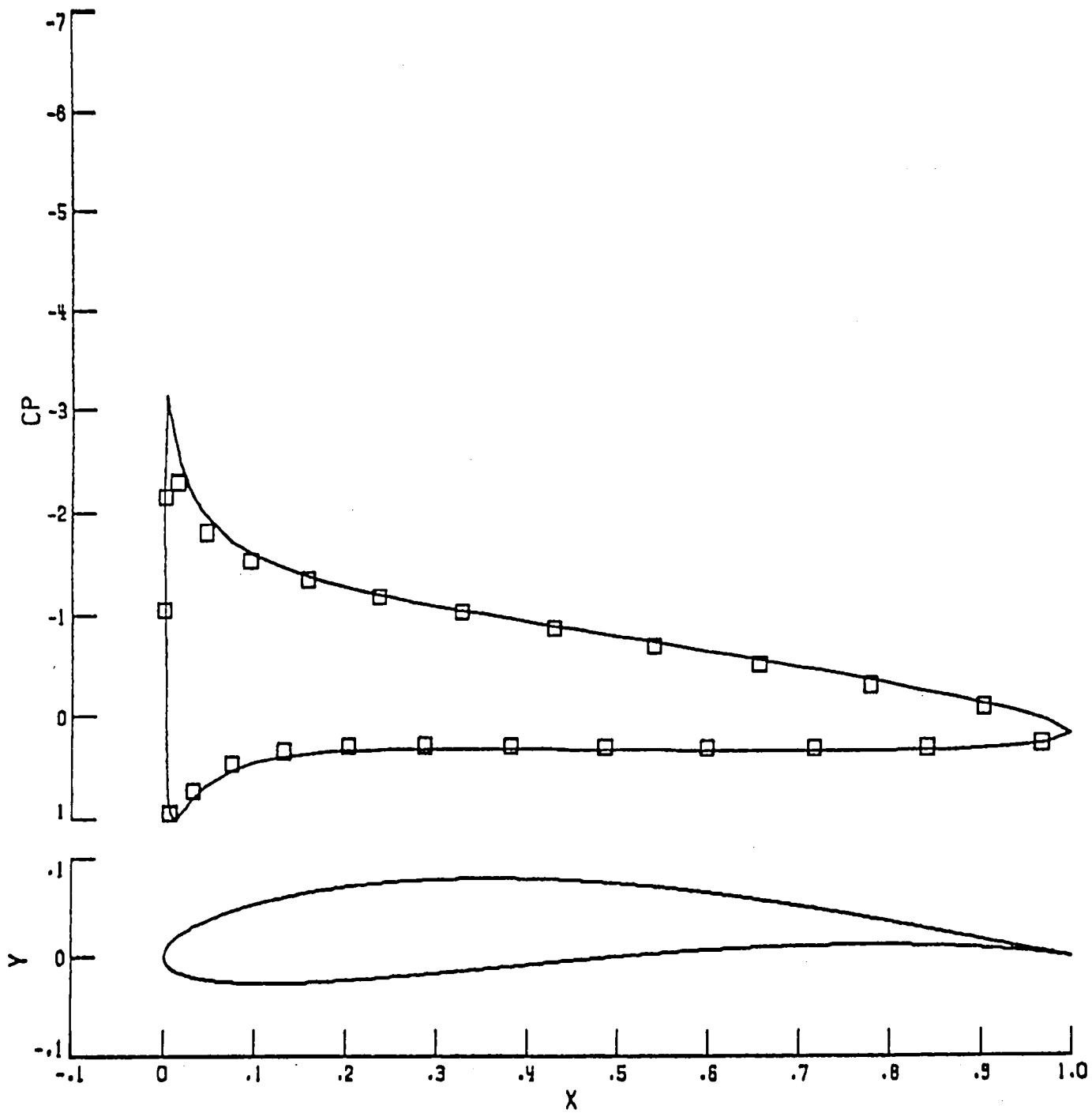


Figure 6d

### Figure Captions

1. An axially symmetric body immersed in a uniform stream, with an indication of the coordinate system and the region of the singularity distribution.
2. Pressure coefficient  $C_p(x)$  for an ellipsoid of revolution with  $S(x) = 4x(1 - x)$  and (a)  $\epsilon = 0.1$  and (b)  $\epsilon = 0.2$ . The solid line represents the perturbation solution, "o" represents the exact solution, and " $\square$ " represents the numerical solution.
3. Pressure coefficient  $C_p(x)$  for a dumbbell shaped body with  $S(x) = 12x(1 - x)[1 - 3x(1 - x)]$  and (a)  $\epsilon = 0.03$  and (b)  $\epsilon = 0.07$ . The solid line represents the perturbation solution and " $\square$ " represents the numerical solution. The profile shape of the body is indicated at the bottom of each figure.
4. A two-dimensional airfoil immersed in a uniform stream, with an indication of the coordinate system and the endpoints ( $\alpha$  and  $\beta$ ) of the line singularity distribution.
5. Pressure coefficient  $C_p(x)$  for a symmetric Joukowski airfoil with  $C(x) \equiv 0$  and  $S(x) = x(1 - x)^3$  and angle of attack  $\gamma = 6^\circ$  for (a)  $\epsilon = 0.01624$  and (b)  $\epsilon = 0.04872$ . The solid line represents the perturbation solution while " $\square$ " represents the numerical solution.

6. Pressure coefficient  $C_p(x)$  calculated from the perturbation solution (solid line) and the panel method ( $|\square|$ ) for a cambered second-order Joukowski airfoil with  $C(x) = x(1 - x)$ ,  $S(x) = x(1 - x)^3$ , and
- (a)  $\gamma = 0^\circ$ ,  $\epsilon = 0.02688$ ; (b)  $\gamma = 0^\circ$ ,  $\epsilon = 0.08064$ ; (c)  $\gamma = 6^\circ$ ,  $\epsilon = 0.02688$ ; and (d)  $\gamma = 6^\circ$ ,  $\epsilon = 0.08064$ .





1. Report No. NASA CR-172485 ICASE Report No. 84-56		2. Government Accession No.		3. Recipient's Catalog No.	
4. Title and Subtitle COMPARISON OF UNIFORM PERTURBATION SOLUTIONS AND NUMERICAL SOLUTIONS FOR SOME POTENTIAL FLOWS PAST SLENDER BODIES				5. Report Date October 1984	
				6. Performing Organization Code	
7. Author(s) Tin-Chee Wong, C. H. Liu, and James Geer				8. Performing Organization Report No. 84-56	
9. Performing Organization Name and Address Institute for Computer Applications in Science and Engineering Mail Stop 132C, NASA Langley Research Center Hampton, VA 23665				10. Work Unit No.	
				11. Contract or Grant No. NAS1-17070	
12. Sponsoring Agency Name and Address National Aeronautics and Space Administration Washington, D.C. 20546				13. Type of Report and Period Covered Contractor Report	
				14. Sponsoring Agency Code 505-31-83-01	
15. Supplementary Notes Langley Technical Monitor: J. C. South, Jr. Final Report					
16. Abstract  Approximate solutions for potential flow past an axisymmetric slender body and past a thin airfoil are calculated using a uniform perturbation method and then compared with either the exact analytical solution or the solution obtained using a purely numerical method. The perturbation method is based upon a representation of the disturbance flow as the superposition of singularities distributed entirely within the body, while the numerical (panel) method is based upon a distribution of singularities on the surface of the body. It is found that the perturbation method provides very good results for small values of the slenderness ratio and for small angles of attack. Moreover, for comparable accuracy, the perturbation method is simpler to implement, requires less computer memory, and generally uses less computation time than the panel method. In particular, the uniform perturbation method yields good resolution near the regions of the leading and trailing edges where other methods fail or require special attention.					
17. Key Words (Suggested by Author(s))  perturbation methods, panel method, pressure coefficient			18. Distribution Statement  02 - Aerodynamics 34 - Fluid Mechanics & Heat Transfer 64 - Numerical Analysis  Unclassified - Unlimited		
19. Security Classif. (of this report) Unclassified		20. Security Classif. (of this page) Unclassified		21. No. of Pages 33	22. Price A03

For sale by the National Technical Information Service, Springfield, Virginia 22161

